ScienSage

Journal of Advanced Scientific Research

Available online through http://www.sciensage.info

ISSN
0976-9595
Research Article

NANOFIBRILLATED CELLULOSE/ACRYLONITRILE BUTADIENE RUBBER COMPOSITES: MORPHOLOGY, MECHANICAL AND DYNAMIC MECHANICAL PROPERTIES

Gean A. Varghese[1, 2], Dileep P.[1], Sunil K. Narayanankutty*[1]

[1]*Department of Polymer Science and Rubber Technology, Cochin University of Science and Technology (CUSAT), Kerala, India*

[2]*Department of Chemistry, St. Peter's College, Kolenchery, Kerala, India*

**Corresponding author: sncusat@gmail.com*

ABSTRACT

Cellulose fibre isolated from agricultural waste material, tapioca stem by physico-chemical method was subjected to a size reduction process to produce nanofibers of average fibre width of 50 nm. This was used to prepare acrylonitrile butadiene rubber (NBR) composite by wet masterbatch technique. Wet masterbatch technique is an eco-friendly process which is more effective compared to the reported dry rubber compounding procedures since colloidal dispersion of polar cellulose fibres are mixed with NBR latex (aqueous dispersion) so as to facilitate the interpenetration of the two polymeric phases without the expense of much energy, assistance of costly equipments or compromising on elastomer strength. Masterbatch maximises the interaction between the nanofiller and the matrix which is reflected in the improved mechanical properties. The effect of nanocellulose concentration on the morphology and mechanical and dynamic mechanical properties of the nanocomposites has been studied. Significant improvement in modulus (60%) and tensile strength (112%) of the composite was observed at an optimum fibre loading of 3 phr. The thermal stability of NBR was improved by 19°C and the storage modulus was increased by 6 MPa. Scanning electron microscopy revealed that better dispersion of the nanocellulose was possible by masterbatch method.

Keywords: Nanocellulose, Acrylonitrile butadiene rubber, Masterbatch method, Abrasion resistance, Dynamic Mechanical properties

1. INTRODUCTION

Acrylonitrile butadiene rubber (NBR) is one of the outstanding synthetic elastomer which finds its application in petroleum, automobile, aviation, printing, artificial leather and glove industries [1, 2]. Fillers are used in elastomers to improve its properties and processability. Particle size, surface morphology and chemical functionalities of the filler determine the compatibility and effectiveness of the filler [3-9]. Fibrous fillers constitute a versatile class of filler that is generally used along with elastomers. Rubber composites having nanofibers as reinforcement have several advantages over other macro and micro fibrous composites due to their higher aspect ratio [10-12]. Considering the depletion of natural resources and environmental concerns associated with the refining of petroleum, synthetic fibres like nylon, aramid, rayon etc. are now being replaced by renewable natural fibres [13-15].

Cellulose is the most abundant natural fibre with the universal distribution. The use of lignocellulosic fibres improves the mechanical properties of elastomers [16]. The compatibility and reinforcement of cellulose fibres increase when cellulose nanofibers are used [17]. Cellulose nanofibre from different sources and geographic regions shows different morphology and aspect ratio [17-19]. Cao et al. have studied the composite of commercial cotton linter pulp and NBR and found that the glass transition temperature (Tg), the storage modulus and the degradation temperature increased. However, they have not considered the effect of nanocellulose at the lower concentration which is very much significant in the case of nanofillers [20]. Suryani et al. have used commercially available nanocrystalline cellulose to prepare NBR composites and found improvement in the thermal stability of the composite [21]. But they employed the solution casting technique which is less significant in the case of industrial application. Melt blending method has been successfully applied by Verge et al. for the preparation of acrylonitrile butadiene rubber/Carbon nanotube composites [22]. Wu

et al. prepared NBR/clay nanocomposites by the co-coagulating method and found an excellent gas barrier properties [23]. Roy et al. studied the effect of surface modified nano calcium carbonate and extender linseed oil on the mechanical properties of NBR nanocomposites [24]. Nurul et al. modified nanocellulose by acetylation process and investigated its dispersibility and reinforcing efficiency in NBR nanocomposites [25]. Different techniques were used to incorporate the fillers into the elastomer matrix of which dry mixing and solution casting were most common [22, 23, 26]. In our previous work it was reported that dry mixing was more effective than solution casting in enhancing the properties of natural rubber blend. The properties of a composite will be improved as the filler becomes more compatible and one of the ways for that is to attain a uniform distribution. Latex is an emulsion of colloidal rubber molecules stably distributed in an aqueous phase. Wet masterbatch technique is used to increase the dispersibility of cellulose inside the elastomer since colloidal nanocellulose fibres dispersed in aqueous medium can distribute itself well in latex. The conventional dry mixing process is more laborious and energy consuming and needs higher mixing time and reduces the molecular weight of the polymer whereas the wet masterbatch technique is a highly eco-friendly process with simplified mixing process, reduced energy intake and reduced polymer chain fission due to the mild conditions of mixing [27-29]. Film drying technique was preferred over co-coagulation since coagulation destabilises the cellulose dispersion which may cause agglomeration of cellulose fibres [30].

In this work, the results of studies on nanocellulose/NBR composite prepared in masterbatch form (refer graphical abstract) at different fibre concentrations to get improved interaction between NBR and nanocellulose are reported. The composites vulcanised using conventional vulcanizing agents were evaluated for morphology, mechanical properties and thermal degradation characteristics. It was found that the nanocellulose fibres isolated from agricultural waste material, tapioca stem has great potential in the fabrication of NBR nanocomposites.

2. MATERIAL AND METHODS

2.1. Raw materials

Nitrile Butadiene Rubber latex (Encord, 40% DRC) was kindly supplied by Jubilant industries Noida, India. Nanocellulose fibres prepared in our laboratory from Tapioca stems with an average diameter of 50 nm. All other chemicals viz. zinc oxide (ZnO), stearic acid, 1,2-dihydro2,2,4-trimethylquinoline (TQ), N-cyclohexyl-2-benzothiazole sulphenamide (CBS), Tetramethylthiuram Disulfide (TMTD) and sulphur (S) were of commercial grade.

2.2. Methods

2.2.1. Preparation of NBR/Nanocellulose masterbatch

The requisite amount of nanocellulose dispersion (1-5 phr) was added dropwise to NBR latex followed by continuous stirring for 1 hour at 2000 rpm using a mechanical stirrer. After thorough stirring, the mixture was poured into a glass tray for film casting. Film casting was done by placing the glass tray in a hot air oven at 60°C temperature for 24 hours. The films were separated and cut into rectangular pieces and dried again at 50°C till constant weight. The dried masterbatch films were used for final compounding.

2.2.2. Preparation of NBR/Nanocellulose composites

The dried masterbatch was compounded according to American Society for Testing and Materials standards [ASTM D 3184] as per the formulation given in Table 1 on a Thermo Haake Polylab (QC Version 1.02), an internal mixer equipped with Banbury rotors at 60°C and 60 rpmfor 7 minutes.

Table1: Formulation of NBR/Nanocellulose compounds

Ingredients *	Mix Names					
	NBR Gum	NBR 1C	NBR 2C	NBR 3C	NBR 4C	NBR 5C
NBR latex (40% DRC)	250	250	250	250	250	250
Nanocellulose (phr)[a]	0	1.0	2.0	3.0	4.0	5.0

** Sulphur 2.5, Zinc oxide 4.0, Stearic acid 2.0, 1,2-dihydro2,2,4-trimethylquinoline 1.0, Tetramethylthiuramdisulfide (TMTD) 0.1 and N-cyclohexyl-2-benzothiazole sulphenamide 0.9 (all in phr) were common to all formulations.[a] parts per hundred rubber*

NBR nanocellulose masterbatch was masticated for 3 minutes for the molecular break down and then elemental sulphur is added to it followed by ZnO and stearic acid. After 2 minutes TQ and CBS were also added to the mix. Mixing was continued for 2 more minutes for homogeneous distribution of all ingredients in NBR. After mixing, the compound was passed 6 times through a tight nip gap on a laboratory two-roll mixing mill (size 6"x12") and finally sheeted out at a nip gap of 3mm. The compound was kept at room temperature for 24 hours for maturation. The cure time was determined in a rheometer (RPA 2000) using approximately 5 g sample. The test specimens were vulcanized at 150°C for optimum cure time in standard moulds by compression moulding using an electrically heated hydraulic press with 12"x12" platen size at a pressure of 150 kg/cm^2.

2.3. Characterization methods

Rheological characteristics were determined by using Rubber Process Analyser, RPA 2000 as per ASTM D 5289 [26]. Stress- strain tests were carried on a Shimadzu Model AGI Universal Testing Machine (UTM) as per ASTM D 412. Tear resistance of the samples was tested as per ASTM D 624 using the un-nicked 90° angle test specimen. The hardness of compression moulded samples were measured as per ASTM D 2240 by shore A type Durometer. Bariess DIN abrader was used to test the abrasion resistance (ASTM D 5963). The specific gravity, as per ASTM D 297, was determined using a Densimeter. Wallace Dunlop Tripsometer was used to measure the rebound resilience according to ASTM D 7121. Percentage of rebound resilience (RB) was calculated using the equation:

$$RB = \frac{1-\text{Cos (angle of rebound)}}{1-\text{Cos (original angle)}} X100 \quad \ldots\ldots\ldots\ldots\ldots\ldots 1$$

Thermogravimetric analysis was performed on Thermogravimetric Analyzer Q-50, TA instruments with a heating rate of 20°C/min under nitrogen atmosphere. DMAQ800 dynamic mechanical analyzer was used for dynamic mechanical analysis of the samples in tension mode. The fracture surfaces of the samples were studied with JOEL JSM 8390 LV scanning microscope.

3. RESULTS AND DISCUSSION

3.1. Cure characteristics of NBR/Nanocellulose compounds

Cure curves of NBR gum and NBR/Nanocellulose compounds are shown in Fig. 1. The rheological data obtained from RPA is presented in Table 2. The cure characteristics provide an idea about the processability of the compounds. Cure parameters are affected by the amount of filler added its morphology and state of aggregation [27].

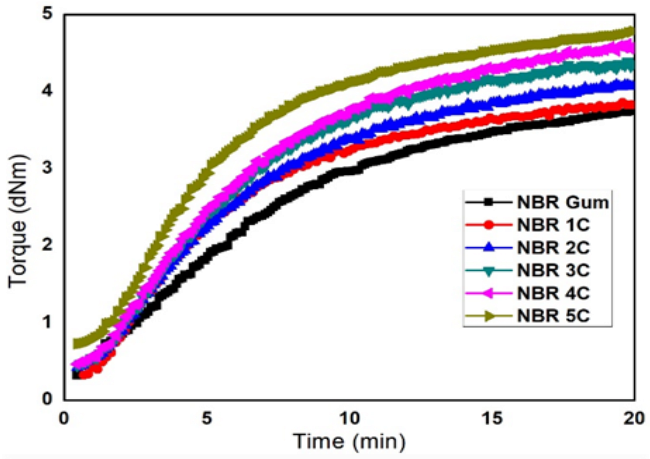

Fig.1: Cure curves of NBR/Nanocellulose compounds

Table 2.Rheological data of NBR/Nanocellulose compounds

Sample name	t_{10} (min)	t_{90} (min)	M_L (dNm)	M_H (dNm)	M_H-M_L (dNm)	CRI (min^{-1})
NBR	1.3	13.6	0.3	3.8	3.4	8.2
NBR 1C	1.1	12.6	0.3	3.9	3.5	8.7
NBR 2C	1.7	13.1	0.4	4.1	3.7	8.8
NBR 3C	1.9	13.1	0.5	4.4	3.9	9.0
NBR 4C	1.9	13.0	0.5	4.6	4.2	8.9
NBR 5C	2.0	11.8	0.7	4.8	4.1	10.3

The minimum torque (M_L) and maximum torque (M_H) values of NBR compounds increase with increasing cellulose nanofibre concentration. The hydroxyl group of the nanocellulose interacts with the Zn^{2+} ions bound in the rubber matrix [28]. This interaction will increase the stiffness of the material which is reflected as the increase

in torque. The scorch time (T_{10}) increases with the increase of nanocellulose loading. This is due to the adsorption of vulcanizing agents by the nanocellulose due to its high surface area [29]. The cure time (T_{90}) increases up to 3 phr and then decreases with further addition of fibres. This indicates that polar rubber can hold much of the compounding ingredients and the heat generated by the movement of fillers activates the cure process [4]. The same explanation holds good for the trend in the differential torque values (M_H-M_L) and cure rate index (CRI) as the differential torque and CRI values increase on the addition of nanocellulose upto 3 phr loadings.

3.2. Morphological analysis

The morphological images of NBR Gum and NBR 3C samples are reported in Figures 2(a) and 2(b), respectively. The tensile fractured surface of NBR Gum is smooth with tiny particles embedded, which may be the curatives. The flat surface of NBR Gum shows a typical fracture mechanism for elastomers. The wrinkles, undulations and deformation areas are seen in Figure 2(b) represent the effective stress transfer in NBR 3C composites.

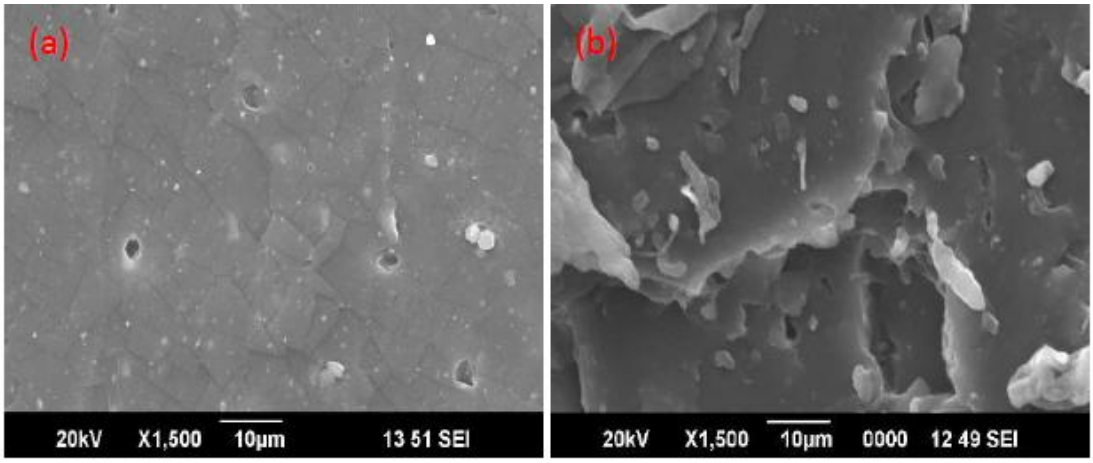

Fig.2: SEM images of tensile fractured surface of (a) NBR Gum and (b) NBR 3C composite

3.3. Dynamic mechanical properties

Figure 3 shows the strain dependence of the storage modulus of NBR Gum and NBR/Nanocellulose nanocomposites. For composites of rubber dynamic properties vary with strain amplitude. This nonlinear behaviour of filled rubber is known as the Payne effect [30], which is responsible for the reduction in storage modulus at higher strain for filled rubbers. The storage modulus values of NBR 3C and NBR 5C composites are 11 MPa and 9 MPa, respectively, which is 120% and 80% higher than that of the NBR Gum compound. An increase in nanocellulose loading leads to an increase in bound rubber content, which increases the effective volume of nanocellulose causing an enhancement in modulus of the rubber [31]. This increase in storage modulus is attributed to the hydrodynamic effect of rigid filler particles. The decrease in storage modulus at 5 phr nanocellulose loading is due to the breaking of the filler-filler network due to agglomeration of nanocellulose fibres at higher loading. The strain sweep plot reveals the agglomeration of nanocellulose fibres above 3 phr and the storage modulus value is in close agreement with the value of modulus at 300% elongation.

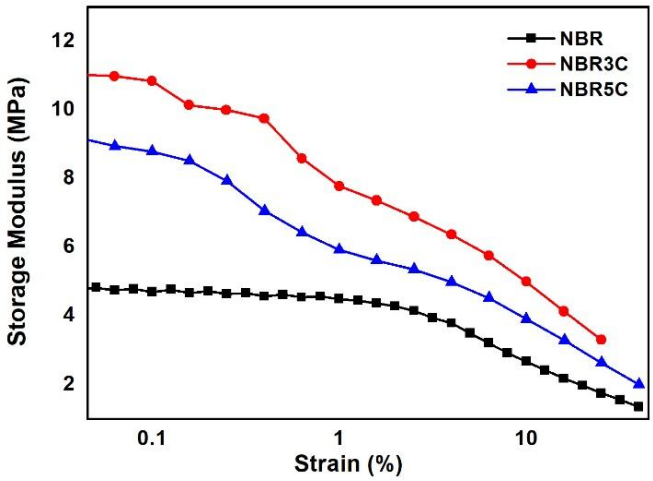

Fig.3: Variation in storage modulus with strain

3.4. Thermogravimetric Analysis

The TG and DTG curves of NBR Gum, NBR 3C and NBR 5C composites are shown in Figure 4. It is clear that all of the three samples have two-step degradation. In

Figure 4(a) the initial weight loss at 200-300°C is related to the degradation of unstable additives such as cross-linking agents and small molecular weight additives [32]. The second step of degradation occurs in the range of 300-475°C, which is attributed to NBR degradation [21]. The thermal degradation characteristics of NBR gum and NBR nanocellulose composites are represented in Table 3. The onset degradation temperature (temperature at 5% degradation) of NBR 3C is 342°C, which is 14°C higher compared to NBR Gum and NBR 5C. This indicates that the thermal stability of NBR composites is greatly influenced by the uniform dispersion of nanocellulose. The residual weight at 750°C (%) is also increased with the filler loading.

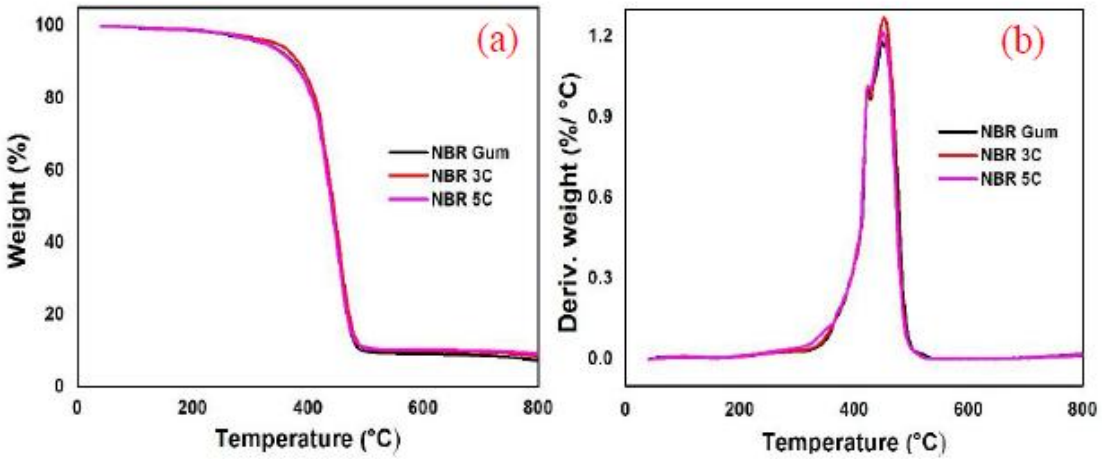

Fig.4: TG and DTG curves of NBR Gum, NBR 3C and NBR 5C composites

Table 3: Thermal degradation characteristics of NBR gum and NBR/Nanocellulose composites

Name of sample	T_{on}, (°C)	T_{max}, (°C)	T_{50}, (°C)	Residue at 750 °C (%)
NBR Gum	328	452	442	8.7
NBR 3C	342	452	444	9.6
NBR 5C	329	452	441	10.1

T_{on} - Onset degradation temperature, T_{max} - Maximum degradation temperature and T_{50}- Temperature at 50% degradation

3.5. Mechanical Properties

3.5.1. Tensile strength

The tensile strength of the composites increases considerably on the addition of nanocellulose to NBR matrix as shown in figure 5. The maximum tensile strength is obtained by the addition of 3 phr nanocellulose to the elastomer after which the strength decreases. The tensile strength of the composite shows an increase of 112% for the 3 phr nanocellulose composite. This improvement in tensile strength is due to the uniform distribution of cellulosic nanofibres obtained by the masterbatch method and may also due to the favourable interaction between hydroxyl group of the nanocellulose and the cyanide group of the NBR matrix. The interaction with polar Zn^{2+} ions and the polar groups on the surface of the nanocellulose fibres also enhances the compatibility of the filler in the matrix.

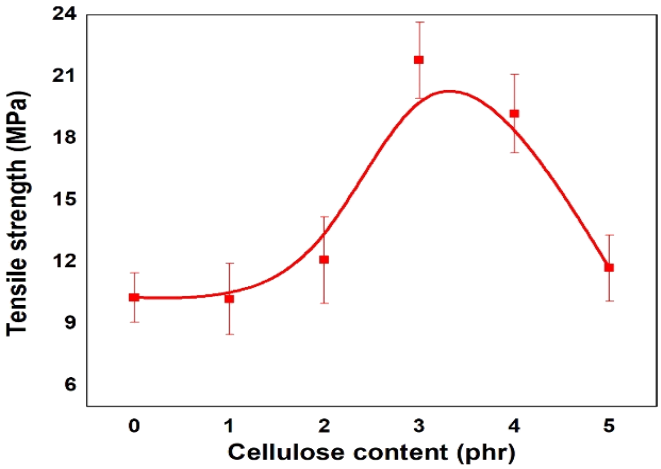

Fig.5: Plot of tensile strength of NBR/Nanocellulose composites

The decrease in tensile strength at higher filler loading is due to the agglomeration of the nanocellulose as reported by Midhun et al. [33] Large agglomerates always disturb the homogeneity of the composite and create stress concentration points which are responsible for the decrease in tensile strength [34].

3.5.2. Modulus at 300% elongation

The addition of nanocellulose to NBR increases the modulus at 300% elongation as shown in Fig. 6. The modulus shows an increase of 60% by the addition of 3 phr nanocellulose after which it remains almost constant. NBR3C shows maximum modulus value since it has got uniform filler dispersion. The increased reinforcement due to hydrogen bond formation between the polar nitrile group of the elastomer and the hydroxyl group of the nanocellulose, increases the rigidity of the nanocomposite [27]. An increase in rigidity is displayed as higher stress value which in turn increases the modulus. After the addition of 3 phr of nanocellulose, agglomeration may take place which hinders the rate of increase of modulus with filler loading.

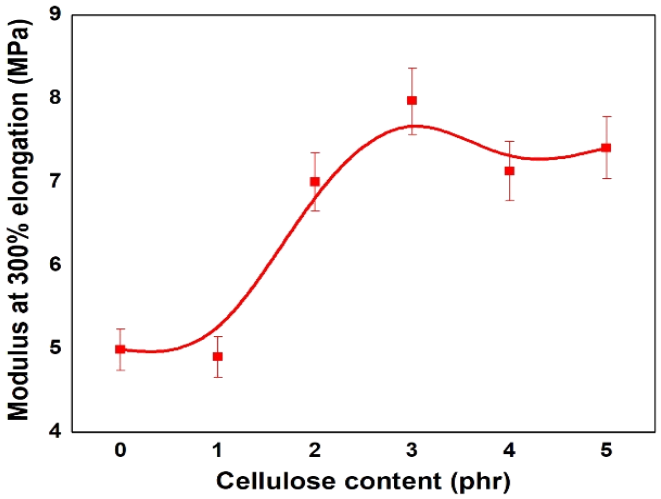

Fig.6: Modulus at 300% elongation

3.5.3. Tear strength

Figure 7 shows the plot of tear strength of NBR/Nanocellulose composites. The tear strength of NBR nanocomposites exhibits an increasing tendency by the addition of nanocellulose upto 3 phr, which is due to the obstruction of tear path by the nanocellulose fibres. The decrease in tear strength at higher concentrations of nanocellulose may be due to the poor rubber filler interaction and filler agglomeration [35].

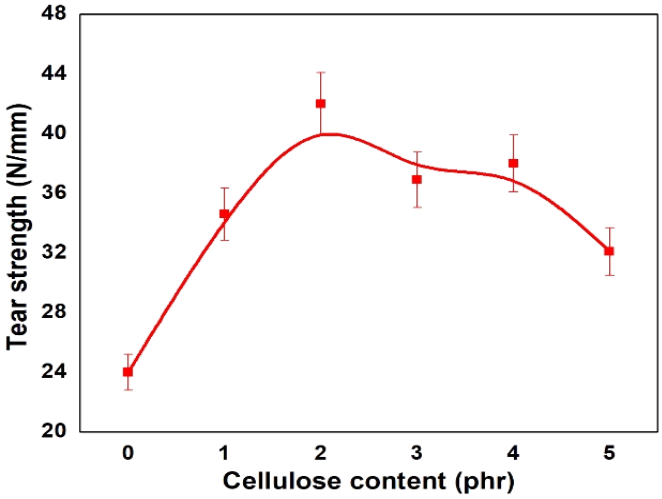

Fig.7: Plot of tear strength of NBR/Nanocellulose composites

3.5.4. Other mechanical properties

The abrasion resistance index (ARI), hardness and rebound resilience of NBR/Nanocellulose composites are tabulated in Table 4.

Table 4: Other mechanical properties

Sample name	Abrasion resistance index (%)	Hardness (shore A)	Rebound resilience (%)
NBR Gum	223±2	55±0.5	75±0.2
NBR 1C	246±3	56±0.5	73.9±0.3
NBR 2C	278±4	57.5±0.5	73.5±0.3
NBR 3C	284±3	59±0.5	73.2±0.3
NBR 4C	239±5	60±1	72.1±0.4
NBR 5C	223±7	60.5±1	70.3±0.4

Abrasion resistance index is the key parameter that determines the service life of the composites. ARI is increased up to 3 phr nanocellulose loading and then decreased. At higher rubber-filler interactions the dislodgement of the vulcanizates under abrasion will be more difficult. The decrease in ARI indicates the agglomeration of nanocellulose in NBR composites. The hardness of all composite increased with increasing nanocellulose loading as reported by Schueneman et al. [36]. The maximum hardness value is 60.5 shore A, which corresponds to 10% increase. The rebound resilience at room temperature decreases with the increase of nanocellulose due to the rigid nature of nanocellulose. The percentage rebound resilience is directly proportional to the modulus of the composites,

and the results of modulus clearly indicate the same. Rebound resilience depends on the uniform dispersion of filler in the matrix, hence a significant change is observed in higher nanocellulose loading in NBR composites [37].

4. CONCLUSIONS

Cellulose nanofibers/NBR composite was prepared through masterbatch route. The optimum fibre loading was 3 phr, as revealed by the results of tensile strength, modulus and abrasion resistance index. Dynamic mechanical analysis indicated that Payne effect was less significant up to 3 phr of nanocellulose. SEM micrographs of the tensile fractured surface of NBR 3C composite showed uniform dispersion of filler in the rubber matrix. Thermogravimetric analysis showed significant improvement in thermal stability by the incorporation of 3 phr nanocellulose in NBR. Hence this masterbatch method of nanocellulose dispersion in NBR latex improve the overall performance of composites and can be used for industrial applications such as oil seals, gaskets etc.

5. REFERENCES

1. Schwartz, M. Encyclopedia of Materials, Parts and Finishes.: CRC Press; 2002.
2. Mishra, M. Encyclopedia of Polymer Applications 3 Volume Set: Chapman and Hall/CRC; 2018.
3. O'Connor, JE. *Rubber Chem. Technol.*, 1977; **50**:945-958.
4. Rajesh C, Unnikrishnan G, Purushothaman E, Thomas S. *J. Appl. Polym. Sci.,* 2004; **92**:1023-1030.
5. Liu J, Gao Y, Cao D, Zhang L, Guo Z. *ACS Sustain. Chem. Eng.*, 2020; **8:**5091-5099.
6. Liu, J., Gao, Y., Cao, D., Zhang, L., Guo, Z. *Langmuir*, 2011; **27:**7926-7933.
7. Tao H, Dufresne A, Lin N. *Macromolecules*, 2019; **52:**5894-5906.
8. Sinclair A, Zhou X, Tangpong S, Bajwa DS, et al. *ACS Omega,* 2019; **4:**13189-13199.
9. Parambath Kanoth B, Claudino M, Johansson M, Berglund LA, et al. *ACS Appl. Mater. Interfaces*, 2015; **7:**16303-16310.
10. Mathew L, Narayanankutty SK.. *Polym. Plast. Technol. Eng.*, 2008; **48:**75-81.
11. Wang F, Feng L, Tang Q, Liang J, et al. *J. Nanomater.* **2013**, doi.10.1155/2013/369409.
12. Medupin RO, Abubakre OK, Abdulkareem AS, Muriana RA et al. *Sci. Rep.,* 2019; **9:**1-11.
13. Siqueira, G., Bras, J. & Dufresne, A. *Polymers (Basel).*, 2010; **2**:728-765.
14. Favier V, Canova GR, Cavaillé JY, Chanzy H, et al. *Polym. Adv. Technol.*, 1995; **6**:351-355.
15. Gopalan Nair, K. & Dufresne, A. *Biomacromolecules*, 2003; **4**:666-674.
16. Parambath Kanoth B, Thomas T, Joseph JM, Narayanankutty SK. *Polym. Compos.*, 2019; **40**:414-423.
17. Bras J, Hassan ML, Bruzesse C, Hassan EA, et al. *Ind. Crops Prod.,* 2010; **32:**627-633.
18. Trovatti E, Carvalho AJF, Ribeiro SJL, Gandini A. *Biomacromolecules*, 2013; **14**:2667-2674.
19. Visakh PM, Thomas S, Oksman K, Mathew AP. *Compos. Part A Appl. Sci. Manuf.*, 2012 ;**43**:735-741.
20. Cao X, Xu C, Wang Y, Liu Y, et al. *Polym. Test.*, 2013; **32**:819-826.
21. Suryani E, Rashid A, Binti N, Julkapli M, et al. *J. Appl. Polym. Sci.*, 2018; **135:**46594 1-9.
22. Verge P, Peeterbroeck S, Bonnaud L, Dubois P. *Compos. Sci. Technol.*, 2010; **70**:1453-1459.
23. Wang Y, Zhang H, Wu Y, Yang J, et al. *J. Appl. Polym. Sci.,* 2005; **96**:318-323.
24. Roy K, Alam N, Debnath SC. *Int. J. Innov. Res. Sci. Eng.*, 2014; **2:**69-75.
25. Nurul M, Mohammad A, Yehye WA, Julkapli NM, et al. *Fibers Polym.*, 2018; **19**:383-392.
26. Standard Test Method for Rubber Property; Annual Book of ASTM Standards: ASTM International; D 5289;1995.
27. Chen Y, Zhang Y, Xu C, Cao X. *Carbohydr. Polym.*, 2015; **130**:149-154.
28. Abraham E, Deepa B, Pothan LA, John M, et al. *Cellulose*, 2013; **20**:417-427.
29. Dileep P, Narayanankutty SK. *Mater. Today Commun.,* 2020; **24**:100957.
30. Stöckelhuber KW, Svistkov AS, Pelevin AG, Heinrich G. G. *Macromolecules*, 2011; **44:**4366-4381.
31. Das A, Jurk R, Stöckelhuber KW, et al. *J. Macromol. Sci. Part A Pure Appl. Chem.,* 2009; **46**:7-15
32. Shao L, Ji ZY, Ma JZ, Xue CH, et al. *Sci. Rep.,* 2016; **6**; 1-14.
33. Dominic MCD, Joseph R, Begum PMS, Meera Joseph, et al. *Polymers (Basel).*, 2020; **12**:814.
34. Padmanabhan D., Narayanankutty SK. *Polym. Test.*, 2020; **82**:106302.
35. Dominic M, Joseph R, Sabura Begum PM, Kanoth BP, et al. *Carbohydr. Polym.*, 2019; **230**:115620 doi:10.1016/j.carbpol.2019.115620.
36. Schueneman GT, Lesser AJ, Hobbs TR, Novak BM. *J. Polym. Sci. Part B Polym. Phys.,* 1999; **37**:2601-2610.
37. Datta J, Kosiorek P, Włoch M. *Iran. Polym. J.*, 2016; **25**:1021-1035.